

The Corrosion Behavior of Sputter-deposited Ternary Zr-(12-18)Cr-W Alloys in 12 M HCl Solution

*Jagadeesh Bhattarai**

Central Department of Chemistry, Tibhuvan University, GPO Box 2040, Kathmandu, Nepal
e-mail: bhattarai_05@yahoo.com

Abstract

Ternary amorphous or/and nanocrystalline Zr-(12-18)Cr-W alloys were successfully prepared by direct current (DC) magnetron sputtering. The corrosion rates of Zr-(12-18)Cr-W alloys are in the range of $1-2 \times 10^{-3}$ mm/y which are even lower than those of the sputter-deposited binary W-Zr and W-Cr alloys, and are nearly one order of magnitude lower corrosion rate than those of the alloy-constituting elements in 12 M HCl at 30°C, open to air. All the examined sputter-deposited amorphous or/and nanocrystalline Zr-(12-18)Cr-W alloys are passivated spontaneously. The zirconium addition suppresses the anodic dissolution current, and hence the anodic current densities of the alloys decreased with increasing the zirconium content in the alloys. It is, therefore, considered that the simultaneous additions of zirconium and tungsten with 12-18 at% of chromium enhance synergistically the corrosion-resistant and pitting corrosion of the sputter-deposited Zr-(12-18)Cr-W alloys in 12 M HCl.

Keywords: *Corrosion-resistant, Zr-Cr-W alloys, electrochemical measurement, pitting corrosion*

Introduction

The sputter deposition is used as one of the potential methods for preparation of corrosion-resistant amorphous or nanocrystalline alloys, and this technique is known to form amorphous or nanocrystalline structures over the widest composition range. Therefore, the use of sputter deposition is becoming a quite suitable method for tailoring the corrosion-resistant alloys for last two decades. Even if amorphous alloys are not formed by the sputter deposition, alloys thus prepared are always composed of nanocrystals with very fine grains and sometimes behaves similar to the single-phase amorphous alloys. The single-phase nature of amorphous or nanocrystalline alloys is generally responsible for their high corrosion resistance owing to the formation of uniform protective passive films those are able to separate bulk of alloys from aggressive environments¹. The sputter-deposited alloys consisting of either amorphous or/and nanocrystalline single-phase are chemically

*Corresponding author

homogeneous, and hence are interesting in the view of corrosion resistance. The present author has been reported that the sputter deposition of tungsten with zirconium^{2,4} and chromium^{3,5-7} was effective in preparing binary amorphous or/and nanocrystalline tungsten–base alloys with a high corrosion resistance. Kim et al.⁸ have been reported that the sputter–deposited amorphous Cr–Zr alloys showed high corrosion resistance than those of alloy–constituting elements in aggressive 6 M HCl solution at 30°C. The high corrosion resistance of these sputter-deposited binary tungsten–base and Cr–Zr alloys was based on the spontaneous passivation in aggressive environments.

Chromium, zirconium and tungsten are regarded as very effective alloying elements for enhancing the corrosion resistance of alloys in aggressive environments. In particular, chromium is one of the most effective alloying elements to provide a high passivating ability for conventional steels and stainless steels. Hashimoto reported that the pitting potential of austenitic stainless steels shifted to higher anodic potentials with increasing chromium content of the surface film¹. It has been also reported that only small amount of tungsten addition (that is, less than 10 at%) was enough to cause spontaneous passivation of the sputter–deposited W–Cr alloys even in 12 M HCl and these alloys showed about five orders of magnitude lower corrosion rate than the corrosion rate of chromium metal, and about one order of magnitude lower corrosion rate than that of tungsten^{3,5-7,9}. On the other hand, zirconium is also corrosion–resistant in acidic environments, although it suffers pitting corrosion by anodic polarization. The alloying of zirconium with aluminum¹⁰, chromium⁸ and molybdenum¹¹ greatly improved the corrosion resistance of the alloys in aggressive environments. Similarly, it has been reported that the corrosion resistance of the sputter–deposited amorphous or/and nanocrystalline W–Zr alloys were passivated spontaneously and observed significantly high corrosion resistance in aggressive environments^{2,4}. The corrosion–resistant of the sputter–deposited W–Zr alloys is higher than those of tungsten and zirconium, and hence tungsten addition greatly enhanced the pitting corrosion resistance of zirconium in 12 M HCl^{2,3}.

Furthermore, chromium and tungsten have different characteristics in corrosion behavior, especially in pitting corrosion. Chromium and tungsten are known to be effective elements in improving the pitting corrosion resistance of the alloys, whereas zirconium suffers pitting corrosion by anodic polarization in aggressive chloride–containing environments. The immunity to pitting corrosion is one of the most interesting characteristics of alloys. It has been reported that the synergistic improvement in the resistance to passivity breakdown in chloride–containing media was observed when chromium and zirconium were added simultaneously to the sputter–deposited Mn–Zr–Cr alloys instead of single addition of zirconium or chromium metals¹². In accordance with these facts, if zirconium with chromium and tungsten forms single–phase solid solutions of ternary Zr–Cr–W alloys by sputter deposition, they might be highly corrosion resistance in aggressive 12 M HCl solution. In this context, the present research work is aimed to prepare corrosion–resistant Zr–(12–18)Cr–W alloys with 10–80 at% tungsten content by the sputter deposition method, and to clarify the effects of chromium and tungsten additions on the corrosion behavior as well as the passivity breakdown of the ternary Zr–(12–18)Cr–W alloys in 12 M HCl solution at 30°C, open to air.

Experimental Methods

The DC magnetron sputtering was used for the preparation of the ternary amorphous or nanocrystalline Zr-(12–18)Cr–W alloys. The target was composed of a 99.95% pure zirconium disk of 100 mm diameter and 6 mm thickness, on the erosion region of which 99.95% pure chromium and tungsten disks of 20 mm diameter each were symmetrically placed. The composition of the sputter deposits was changed by changing the numbers of chromium and tungsten disks on the zirconium disk. Glass plates were used as substrates which were rinsed by immersion in water containing a commercial detergent for cleaning at about 75°C. The sputtering apparatus and conditions used were the same as those described elsewhere³.

An electron probe microanalysis (EPMA) was used to determine the composition of the sputter deposits. The structure of the sputter-deposited Zr–Cr–W alloys was confirmed by glancing incident X–ray diffractometer with CuK_α radiation at θ –2 θ mode. The apparent grain size of the alloys was estimated from the full width at half maximum (FWHM) of the most intense reflection according to Scherrer's relation¹³, $t = 0.9\lambda/\beta\cos\theta$, where t is the apparent grain size (in nm), λ is the X–ray wavelength (= 0.15148 nm for CuK_α), β is the FWHM in radian and θ is the diffraction angle of the most intense peak.

Prior to corrosion tests and electrochemical measurements, the surface of the alloy specimens was polished mechanically with silicon carbide paper up to grit No. 1500 in cyclohexane, rinsed with acetone and dried in air in order to obtain reproducible results by removal of the air–formed oxide film formed on as–sputtered alloys. Corrosion rates of the sputter–deposited amorphous or/and nanocrystalline Zr–Cr–W alloys including zirconium and tungsten metals were estimated from the weight loss after immersion for 216 h in 12 M HCl at 30°C, open to air. For chromium metal, the corrosion rate was estimated after immersion for two hours in 12 M HCl. Potentiodynamic cathodic and anodic polarization curves were measured in 12 M HCl at 30°C, open to air after immersion for 24 h when the open circuit potential became almost steady. A platinum mesh and a saturated calomel electrode (SCE) were used as counter and reference electrodes, respectively. All the potential given in this paper are relative to SCE.

Results and Discussion

The composition, structure and apparent grain size (AGS) of the sputter–deposited Cr–Zr–W alloys were analyzed by an electron probe microanalysis (EPMA) and X–ray diffraction (XRD) patterns, respectively. Alloy compositions hereafter are all denoted in atomic percentage (at%). The results of the characterization of the ternary Zr–Cr–W alloys are presented in Table 1. The apparent grain size of the sputter–deposited Zr–Cr–W alloys was estimated from the full width at half maximum (FWHM) of the most intense reflection using Scherrer's relation¹³. The apparent grain size of the Zr–(12–18)Cr–W alloys containing 10–57 at% tungsten is of the order of about 1.1–1.4 nm, which is only a little larger than the size of atom groups supposed to exist in liquid metals. Accordingly, the Zr–(12–18)Cr–(10–57)W alloys containing 25–73 at% zirconium are regarded as

amorphous alloys. On the other hand, the apparent grain sizes of the 8Zr–12Cr–80W and 12Zr–15Cr–73W alloys are about 19.8 and 10.4 nm, respectively, and hence characterized as nanocrystalline and the mixture of amorphous and nanocrystalline structures, respectively. Consequently, the sputter–deposited ternary Zr–(12–18)Cr–W alloys consist of single–phase amorphous or/and nanocrystalline solid solutions supersaturated with alloy–constituting elements (that is, zirconium, chromium and tungsten). In this regards, it is noteworthy to mention here that all these ternary Zr–(12–18)Cr–W alloys are regarded to be homogeneous from the corrosion point of view to have a clear insight into the role of alloying tungsten and zirconium metals on the passivity breakdown and corrosion behavior of the alloys in 12 M HCl solution at 30°C.

Table 1: *Chemical composition, structure and apparent grain size (AGS) of sputter–deposited Zr–Cr–W alloys including alloying elements*

Name of alloys/elements	Zr content (at%)	Structure from XRD	AGS (nm)
Zr–15Cr–10W	73	amorphous	1.4
Zr–15Cr–21W	64	amorphous	1.2
Zr–15Cr–31W	54	amorphous	1.1
Zr–18Cr–57W	25	amorphous	1.2
Zr–15Cr73W	12	amor.+ nanocryst.	10.4
Zr–12Cr–80W	08	nanocrystalline	19.8
Zirconium	100	nanocrystalline	23.0
Chromium	–	nanocrystalline	17.5
Tungsten	–	nanocrystalline	20.2

Figure 1 shows the composition–structure diagram of the sputter–deposited binary Cr–Zr⁸, W–Zr², W–Cr⁵ and ternary Zr–(12–18)Cr–W alloys. This figure reveals that both binary and ternary chromium–base alloys are apt to form amorphous structure over a wide composition range, except for the binary W–Cr alloys, which form nanocrystalline single–phase supersaturated solid solutions of tungsten and chromium metals³. Amorphization of the sputter–deposited W–Cr alloys is not favored because both tungsten and chromium do not satisfy the prerequisites for easy formation of the amorphous structure, that is, negative mixing enthalpy¹⁴ and large atomic size difference¹⁵.

Figure 2 shows the corrosion rates of the sputter–deposited Zr–(12–18)Cr–W alloys after immersion for 216 h in 12 M HCl solution at 30°C, open to air. The corrosion rates of the sputter–deposited binary W–Zr and W–Cr alloys, chromium, zirconium and tungsten metals are also shown for comparison. The corrosion rates of all the examined ternary Zr–(12–18)Cr–W alloys, which are composed of either amorphous or/and nanocrystalline phases, are more than five orders of magnitude lower than that of chromium and about one order of magnitude lower than that of sputter–deposited tungsten and zirconium. The corrosion rates of all the sputter–deposited Zr–Cr–W alloys containing 12–18 at% chromium content are almost same and in the range of about 1–2 x 10⁻³ mm/y. Furthermore, the corrosion rates of the Zr–(12–18)Cr–W alloys are lower than those of the corrosion rates of the binary amorphous or/and nanocrystalline W–Zr² and W–Cr⁵ alloys in 12 M HCl at 30°C. It can, therefore, be said that the simultaneous additions of chromium and tungsten to zirconium enhance synergistically the corrosion resistance of the sputter–deposited Zr–Cr–

W alloys in comparison with the single addition of zirconium or tungsten in 12 M HCl at 30°C.

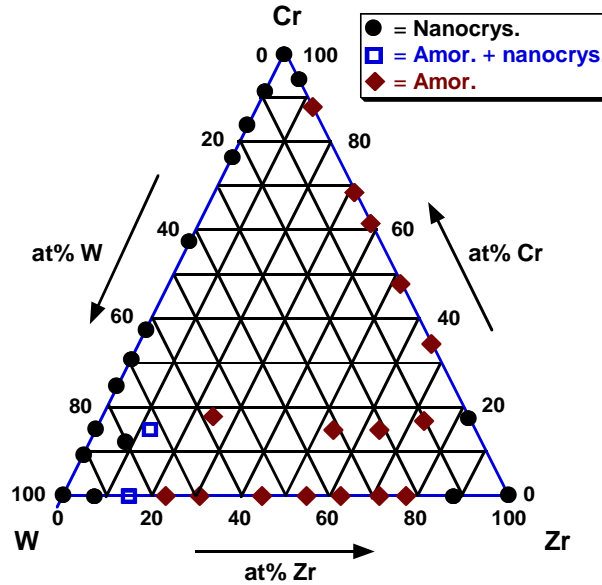


Figure 1: Composition-structure diagram of the sputter-deposited Zr-(12-18)Cr-W alloys including binary Cr-Zr, W-Cr and W-Zr alloys

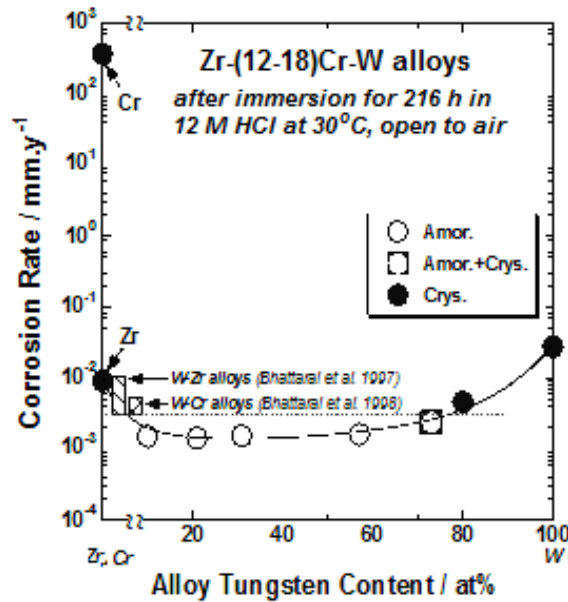


Figure 2: Corrosion rates of the sputter-deposited Zr-(12-18)Cr-W alloys including those of zirconium, chromium and tungsten after immersion for 216 h in 12 M HCl at 30°C, open to air. The corrosion rates of the sputter-deposited W-Zr² and W-Cr⁴ alloys are also shown for comparison

Electrochemical measurements were carried out for a better understanding of the corrosion behavior and passivity of the sputter-deposited Zr–Cr–W alloys. Figure 3 shows the changes in open circuit potentials (OCPs) for Zr–(12–18)Cr–W alloys including the sputter-deposited zirconium, chromium and tungsten metals in 12 M HCl solution at 30°C, as a function of alloy tungsten content. The OCPs of the ternary Zr–Cr–W alloys are located between those of zirconium and tungsten as well as chromium, but are close to that of tungsten. In general, the OCPs of the Zr–(12–18)Cr–W alloys are shifted to more negative direction with increasing zirconium content. Consequently, tungsten addition seems to be effective to ennoble the OCPs of the ternary Zr–(12–18)Cr–W alloys in 12 M HCl solution at 30°C, open to air. Although the open circuit potential of the alloys is shifted to more negative direction with increasing the zirconium content in the alloys, the corrosion rates of the alloys are almost independent with zirconium content in the Zr–(12–18)Cr–W alloys (Fig. 2).

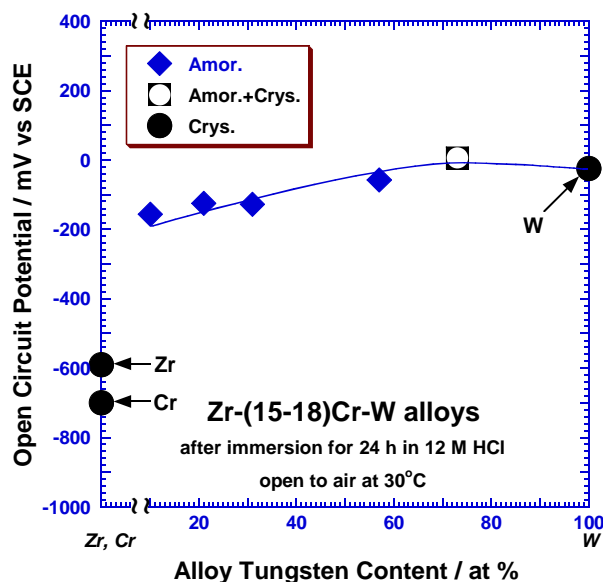


Figure 3: Changes in open circuit potentials for the sputter-deposited Zr–(12–18)Cr–W alloys after immersion for 24 h in 12 M HCl at 30°C, as a function of alloy tungsten content

In order to examine the effects of zirconium, chromium and tungsten contents on the passivity of the alloys, the potentiodynamic polarization curves of the amorphous Zr–Cr–W alloys containing almost the same chromium content (that is, 12–17 at% chromium) are measured (Fig. 4). The cathodic and anodic polarization curves for the sputter-deposited zirconium, chromium and tungsten metals are also shown for comparison. Spontaneous passivation occurs for all the examined sputter-deposited Zr–(12–17)Cr–W alloys in a wide potential region until the onset of transpassive dissolution of chromium metal. The chromium shows the active–passive transition and transpassive dissolution in 12 M HCl. The sputter-deposited zirconium suffers pitting corrosion after potentiodynamic polarization at about 0.05 V (SCE). The OCPs of the ternary (8–73)Zr–(12–17)Cr–(10–

80)W alloys are located between those of zirconium and tungsten as well as chromium, but are close to that of tungsten also (Fig. 3).

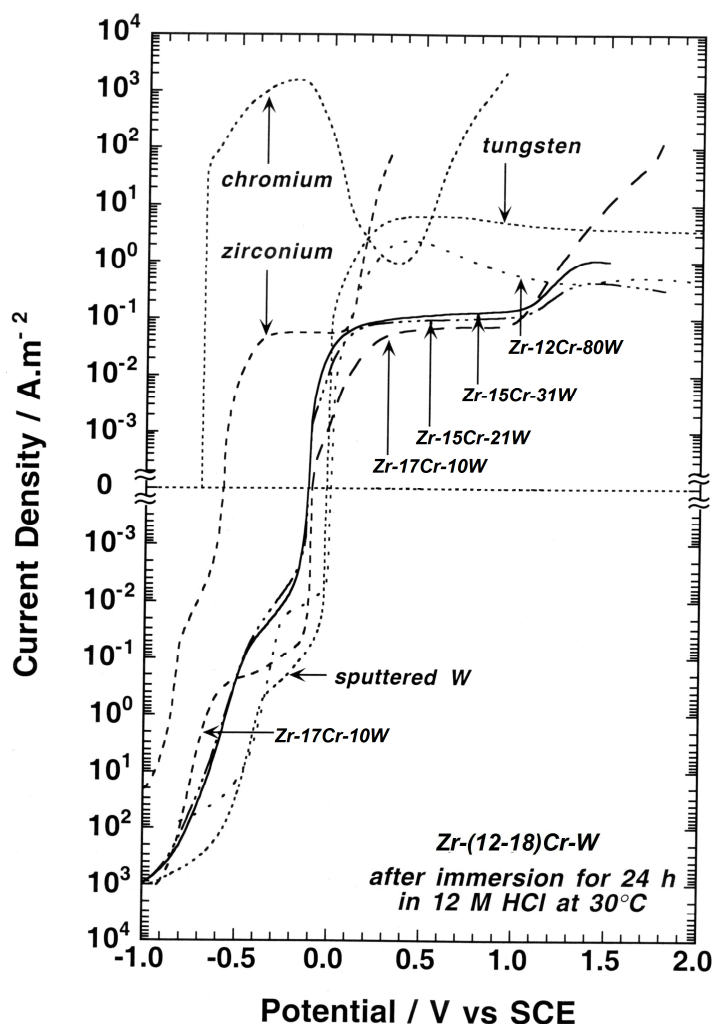


Figure 4: Anodic and cathodic polarization curves for the sputter-deposited Zr-(12–18)Cr–W alloys measured after immersion for 24 h in 12 M HCl at 30°C, open to air. Polarization curves for the sputter-deposited zirconium, chromium & tungsten are also shown for comparison

Anodic passive current densities of the ternary Zr–Cr–W alloys containing 12–17 at% chromium decrease with increasing the zirconium content in the alloys. It is clearly observed that chromium content in both the 54Zr–15Cr–31W and 64Zr–15Cr–21W alloys is exactly same. However, the anodic current density of the 64Zr–15Cr–21W alloy is lower than that of the 54Zr–15Cr–31W alloy in 12 M HCl solution. Consequently, the more effective factor for lowering of the anodic current density of the ternary Zr–Cr–W alloys is mostly due to zirconium as well as tungsten contents. Furthermore, all these four Zr-(12–17)Cr–W ternary alloys containing 10–80 at% tungsten do not suffer pitting corrosion in the

aggressive chloride containing acidic solutions. The abrupt increase in the anodic current density of the Zr-(12–17)Cr–W alloys in the potential region higher than about 1.0 V (SCE) is attributable to transpassive dissolution of chromium. The sputter-deposited binary W–Zr alloys containing 24 at% tungsten or less and pure zirconium metal showed the pitting corrosion in 12 M HCl at 30°C^{2,3}. Furthermore, it has been reported that the sputter-deposited amorphous Cr–Zr alloys containing more than 50 at% zirconium showed the pitting corrosion after potentiodynamic polarization even in 6 M HCl, while the rest of the alloys remained passive until the onset of transpassive dissolution of chromium⁸. Similarly, Mehmood et al.¹⁶ have been reported that the sputter-deposited binary Zr–33Cr alloy showed the pitting corrosion after potentiodynamic polarization at about –0.1 V (SCE) in 6 M HCl. On the other hand, the sputter-deposited Mo–Zr alloys containing 60 at% or more zirconium suffered pitting corrosion by anodic polarization exceeding 1.3 V vs SCE¹¹. In these contexts, it can be said that the addition of only 10 at% tungsten with 12–17 at% chromium in the present study is significantly effective in improving the resistance against the pitting corrosion of the ternary amorphous or/and nanocrystalline Zr–Cr–W alloys in 12 M HCl solution at 30°C.

Conclusions

The Zr–Cr–W ternary alloys containing 12–18 at% of chromium were successfully prepared by D.C. magnetron sputtering and their corrosion behavior was examined in comparison with those of the sputter-deposited binary W–Cr and W–Zr alloys in 12 M HCl solution at 30°C, open to air. The sputter-deposited ternary Zr-(12–18)Cr–W alloys were consisted of single-phase amorphous or/and nanocrystalline solid solutions supersaturated with alloying elements. The Zr-(12–18)Cr–W alloys were passivated spontaneously until the onset of transpassive dissolution of chromium and more protective anodic passive films were formed on the Zr-(12–18)Cr–W alloys with increasing the zirconium content in the alloys. The simultaneous additions of zirconium and tungsten metals to 12–18 at% chromium enhanced synergistically the corrosion-resistant of the ternary Zr-(12–18)Cr–W alloys, and hence these alloys showed higher corrosion resistance than those of alloy-constituting elements. The addition of about 10 at% tungsten with 12–18 at% chromium was significantly effective in improving the resistance against the pitting corrosion of the sputter-deposited Zr-(12–18)Cr–W alloys.

Acknowledgements

The author is very thankful to Professor Emeritus Dr. Koji Hashimoto of Tohoku Institute of Technology, Professor Emeritus Dr. K. Asami of IMR of Tohoku University, Sendai and Professor Dr. H. Habazaki of Hokkaido University, Japan for their kind permission to use the sputtering and XRD machines. Sincere thanks to the Head of Central Department of Chemistry, Tribhuvan University, Kirtipur, Nepal for providing the available research facilities to conduct this research work.

References

1. K. Hashimoto, *In Rapidly Solidified Alloys; Processes, Structure, Properties and Applications* (ed. Howard H. Liebermann), New York: Marcel Dekker, Inc., 1993, p. 591–615
2. J. B. Bhattarai, E. Akiyama, H. Habazaki, A. Kawashima, K. Asami and K. Hashimoto, *Corros. Sci.*, 1997, **39**, 353–375
3. J. Bhattarai, *Tailoring of Corrosion-Resistant Tungsten Alloys by Sputtering*, PhD thesis, Department of Materials Science, Tohoku University, Sendai, Japan. 1998, Pp. 229
4. J. Bhattarai J, A. Kawashima, K. Asami, and K. Hashimoto, In *Proc. 3rd National Confen. Sci. Technol.–1998*; Kathmandu: Nepal Academy of Science and Technology (NAST), 1998, **Vol. 1**, p. 389–407
5. J. B. Bhattarai, E. Akiyama, H. Habazaki, A. Kawashima, K. Asami and K. Hashimoto, *Corros. Sci.*, 1997, **40**, 155–175
6. J. Bhattarai and K. Hashimoto, *Tribhuvan Univ. J.*, 1998, **21(2)**, 1-16
7. J. Bhattarai, *J. Nepal Chem. Soc.*, 2000, **19**, 1–14
8. J-H. Kim, E. Akiyama, H. Habazaki, A. Kawashima, K. Asami and K. Hashimoto, *Corros. Sci.*, 1993, **34**, 1817–1827
9. J. Bhattarai, *J. Instit. Sci. Technol.*, 2002, **12**, 125–138
10. H. Yoshioka, H. Habazaki, A. Kawashima, K. Asami and K. Hashimoto, *Electrochimica Acta*, 1991, **36(7)**, 1227–1233
11. P. Y. Park, E. Akiyama, H. Habazaki, A. Kawashima, K. Asami and K. Hashimoto, *Corros. Sci.*, 1995, **37**, 307–320
12. A. A. El-Moneim, E. Akiyama, H. Habazaki, A. Kawashima, K. Asami and K. Hashimoto, *Mater. Sci. Engg.*, 1999, **A267**, 285–293
13. B. D. Cullity, *Elements of X-ray Diffraction*. 2nd edition, New York, Addison-Wesley Publishing Co., Inc. 1977, p. 101
14. A. K. Niessen, F. R. de Boer, R. Boom, P. F. de Chatel, W. C. M. Mattena and A. R. Miedema, *CALPHAD*, 1983, **7(1)**, 51–70
15. T. Egami and Y. Waseda, *J. Non-Crys. Solids*, 1984, **64**, 113–134
16. M. Mehmood, B. P. Zhang, E. Akiyama, H. Habazaki, A. Kawashima, K. Asami and K. Hashimoto, *Corros. Sci.*, 1998, **40**, 1–18